

Effect of oxygen isotope substitution on the magnetic structure of $(\text{La}_{0.25}\text{Pr}_{0.75})_{0.7}\text{Ca}_{0.3}\text{MnO}_3$

A. M. Balagurov, V. Yu. Pomjakushin,* D. V. Sheptyakov, and V. L. Aksenov

Frank Laboratory of Neutron Physics, Joint Institute for Nuclear Research, 141980, Dubna, Moscow region, Russia

N. A. Babushkina, L. M. Belova, A. N. Taldenkov, and A. V. Inyushkin

RSC "Kurchatov Institute," Kurchatov Square 1, 123182, Moscow, Russia

P. Fischer, M. Gutmann, and L. Keller

Laboratory for Neutron Scattering, ETH Zürich and Paul Scherrer Institute, CH-5232 Villigen PSI, Switzerland

O. Yu. Gorbenko and A. R. Kaul

Department of Chemistry, Moscow State University, 119899 Moscow, Russia

(Received 29 December 1998)

The oxygen isotope effect on the magnetic structure and charge ordering in $(\text{La}_{0.25}\text{Pr}_{0.75})_{0.7}\text{Ca}_{0.3}\text{MnO}_3$ was studied by means of neutron powder diffraction. At first it was found that the two investigated samples, one containing the natural mixture of isotopes (99.7% ^{16}O , metallic at $T \leq 100$ K), and the other one enriched by ^{18}O in 75% (insulating in the whole temperature range), are identical at room temperature. At the temperature lowering the sample with ^{16}O undergoes subsequent antiferromagnetic ($T_{AFM} = 150$ K) and ferromagnetic ($T_{FM} = 110$ K) transitions, while in the sample with ^{18}O pure AFM ordering ($T_{AFM} = 150$ K) is found. The temperature dependencies of the neutron diffraction peak intensities associated with charge ordering are also quite different in the samples with ^{16}O and ^{18}O and correlate with the behavior of the electrical resistivity and the magnetic structure. The temperature behavior of the intensities of the CO and AFM peaks may indicate the presence of phase segregation of the sample with O-16 onto AFM-insulating and FM-metallic phases at low temperature, though no indications of a macroscopic phase segregation were found.

[S0163-1829(99)13025-X]

Recent studies revealed a close interplay of transport and magnetic properties of perovskite manganites $A_{1-x}A'_x\text{MnO}_3$, where $A = \text{La}$, or a rare earth, $A' = \text{Ca}$, Sr , etc. These compounds have been widely known since the discovery of the colossal magnetoresistance (CMR) effect.¹ At room temperature these manganites are usually paramagnetic insulators (PI), and their low temperature state corresponds to a ferromagnetic metal (FMM), or antiferromagnetic insulator (AFI) with a tendency towards charge ordering (CO) of manganese ions (see, for example, Refs. 2–4.) The low temperature state is determined by a subtle balance of several interactions and can be modified by changing the composition or by external forces (pressure or magnetic field). The particular state depends on the doping level, i.e., on the proportion of $\text{Mn}^{3+}/\text{Mn}^{4+}$, and on the relation between the Mn-O and A-O bond lengths which in turn depends on average A-cation radius ($\langle r_A \rangle$).

It is now clear that for the understanding of manganite physics particular attention should be paid to the interplay between their electron and phonon subsystems. A variety of examples evidencing the importance of the electron-phonon interaction are discussed in a recent review,⁵ where this interaction is proposed as a key factor affecting the phase transitions in the CMR compounds. The isotope substitution is a direct experimental method to study the effect of lattice vibrations on physical properties. Several papers have already been published where the strong influence of ^{16}O for ^{18}O substitution on transport and magnetic properties was demonstrated for manganites. In the first papers on this subject

(Zhao and co-workers,^{6,7}) it was found that the Curie temperature decreases by 21 K when 95% of ^{16}O is substituted by ^{18}O in the compounds $\text{La}_{1-x}\text{Ca}_x\text{MnO}_3$ with $x = 0.2$, which significantly exceeds the temperature shifts of magnetic and electronic phase transitions in the other earlier studied oxides such as high-temperature superconductors, and that magnetization and coefficient of thermal expansion of the series strongly depend on the isotope composition. Moreover, a metal-insulator transition induced by oxygen isotope substitution was reported for $(\text{La}_{0.5}\text{Nd}_{0.5})_{0.67}\text{Ca}_{0.33}\text{MnO}_3$ (Ref. 8) and $(\text{La}_{0.25}\text{Pr}_{0.75})_{0.7}\text{Ca}_{0.3}\text{MnO}_3$.^{9,10}

The effect of the oxygen isotope substitution on the ferromagnetic phase transition temperature T_C was studied in Refs. 11,12 for the same series of $\text{La}_{1-x}\text{Ca}_x\text{MnO}_3$ with x in the range from 0.2 to 0.43, and it was shown that the value of the negative shift of T_C evidently depends on $\langle r_A \rangle$. The influence of oxygen isotope substitution on the insulator-metal transition induced by an external magnetic field was studied in Ref. 13. The initial insulating state of $\text{Pr}_{2/3}\text{Ca}_{1/3}\text{MnO}_3$ samples with ^{16}O and ^{18}O isotopes was transformed to a metallic one by applied magnetic field, but in the case of ^{18}O the magnitude of the magnetic field inducing an insulator-metal (I-M) transition was much higher. Ibarra *et al.*¹⁴ have carried out the analysis of the oxygen isotope effect in a $(\text{La}_{0.5}\text{Nd}_{0.5})_{0.67}\text{Ca}_{0.33}\text{MnO}_3$ compound, which, as was found before,⁸ is an insulator down to liquid helium temperatures in the case of ^{18}O , while the ^{16}O sample undergoes the I-M transition at $T \approx 150$ K. The identical sequence of charge

($T_{CO} \approx 210$ K) and magnetic ordering was found for both isotopic samples: FM at $T_{FM} \approx 200$ K and AFM at $T_{AFM} \approx 170$ K.¹⁴ However, a strong difference was observed in the magnetic behavior: The FM contribution to nuclear peak intensities was much lower in the ^{18}O sample than in the ^{16}O specimen.

According to the published data the insulator-metal phase transition is observed in $(\text{La}_{1-y}\text{Pr}_y)_{0.7}\text{Ca}_{0.3}\text{MnO}_3$, with natural oxygen isotope content, for $y \leq 0.75$, while for $y = 1$ the compound is an insulator in the whole temperature range. It was shown in Ref. 10, that the composition with $y = 0.75$ is close to the phase boundary between metal and insulating states, that is conditioned by the critical value of the tolerance factor of the perovskite structure for this compound ($t \approx 0.91$). As a result, the low-temperature state can be easily modified even by a relatively weak effect of the oxygen isotope substitution. It was shown⁹ that the composition with $y = 0.75$ with natural content of oxygen isotopes (99.7% ^{16}O) becomes metallic at $T \approx 100$ K, while the ^{16}O - ^{18}O exchange resulted in the insulating state down to 4 K as had been earlier observed for $(\text{La}_{0.5}\text{Nd}_{0.5})_{0.67}\text{Ca}_{0.33}\text{MnO}_3$.⁸ A possible microscopic model for such a transition was discussed in Ref. 10 in terms of the isotope dependence of the effective electron bandwidth near the I-M phase boundary.

In our previous neutron diffraction study of $(\text{La}_{0.5}\text{Pr}_{0.5})_{0.7}\text{Ca}_{0.3}\text{MnO}_3$ with natural oxygen isotope content,¹⁵ it was shown that the phase transition to the metallic state occurs simultaneously with FM ordering, and is accompanied by a jump in the unit cell volume and ‘‘melting’’ of the orbital ordering of Mn-O bonds. In the present paper we report experimental data obtained for $(\text{La}_{0.25}\text{Pr}_{0.75})_{0.7}\text{Ca}_{0.3}\text{MnO}_3$ by the neutron diffraction technique. Two oxygen isotope samples of this compound have been studied: The first one (O-16 sample hereafter) contained the natural mixture of isotopes (99.7% ^{16}O , metallic at $T \leq 100$ K) and in the other one (O-18 sample hereafter) 75% of oxygen was substituted by ^{18}O (insulating in the whole temperature range.) The main goal of the study was to find out the changes in magnetic structure accompanying the colossal isotope effect in this compound.

The powder samples for neutron diffraction experiments were prepared by means of the so-called ‘‘paper synthesis.’’ In this method an aqueous solution of a mixture of La, Pr, Ca, and Mn nitrates taken in the required ratios was deposited on ash-free paper filters, which were dried (120 °C) and then burned. The oxide product thus obtained was annealed in air at 700 °C for 2 h. The final thermal treatment consisted of annealing pressed pellets in air at 1200 °C for 12 h. Then the pellets were ground and two powder portions of about 5 g weight were placed in alumina boats which were mounted in the furnace inside two quartz tubes. Both samples were treated simultaneously: one sample was heated in natural $^{16}\text{O}_2$ atmosphere, the other one was heated in $^{18}\text{O}_2$ atmosphere (the molar fraction of $^{18}\text{O}_2$ was 85%). The diffusion annealing was carried out at 950 °C under oxygen pressure of 1 bar with enforced circulation of gas. The oxygen atmosphere in the contour was renewed 11 times. The whole time of annealing was 100 h. The final ^{18}O oxygen content in the O-18 sample was $(75 \pm 10)\%$. It was determined from the

weight change and confirmed by mass-spectroscopy analysis of the oxygen atmosphere in the contour.

Neutron diffraction experiments for the magnetic structure determination were carried out on the cold neutron powder diffractometer DMC at the SINQ spallation neutron source at Paul Scherrer Institute (PSI, Villigen). The diffraction patterns were measured by heating the sample from 12 K to 293 K. The samples were packed under a gas atmosphere into cylindrical vanadium containers of diameter 8 mm and 5 cm height. The magnetic structure was refined from the diffraction spectra measured at the wavelength $\lambda = 2.5616$ Å in the range of scattering angles $10^\circ < 2\theta < 90^\circ$, corresponding to interplanar d_{hkl} spacing region from 1.8 to 14.7 Å by the Rietveld method (FULLPROF program,¹⁶ *Pnma* space group).

It is evident that the necessary condition of correct comparison of the results obtained on the samples with isotope substitution is their structural identity. Rietveld refinement of the diffraction patterns at room temperature showed that the O-16 and O-18 samples are indeed identical, in particular with respect to oxygen content with an accuracy of about ± 0.03 . The comparison of the unit cell parameters for both samples gives even better matching for the oxygen content. The unit cell parameters measurement was performed on the time of flight high resolution Fourier diffractometer (HRFD) in Dubna,¹⁷ and gave for room temperature the following results: $a = 5.45657(7)$ Å, $b = 7.69294(9)$ Å, $c = 5.44788(8)$ Å for O-16 and $a = 5.45673(6)$ Å, $b = 7.69315(8)$ Å, $c = 5.44786(7)$ Å for O-18, i.e., the unit cell parameters coincide within an accuracy of (0.002–0.004)%. The comparison of these values with known unit cell parameter dependencies on oxygen content for manganites (see for example Ref. 18) shows that the difference in the oxygen content in O-16 and O-18 samples is less than 0.002. The result of chemical analysis of the O-16 and O-18 samples, performed by an iodometric titration method,¹⁹ is in accordance with this estimation: Oxygen content corresponding to $x = 2.995 \pm 0.008$ in the O-16 specimen, and $x = 2.996 \pm 0.005$ in the O-18 sample for the general formula $(\text{La}_{0.25}\text{Pr}_{0.75})_{0.7}\text{Ca}_{0.3}\text{MnO}_x$.

The neutron diffraction patterns for O-16 and O-18 measured at room temperature on the DMC diffractometer are identical within the reached statistical accuracy (about 50 000 counts in the most intensive peaks). Superlattice reflections such as $(\frac{1}{2}00)$ at $2\theta = 13.6^\circ$ and $(\frac{1}{2}0\frac{1}{2})$ at 19.2° associated with antiferromagnetic (AFM) ordering appeared with decreasing temperature (Fig. 1) for both samples. The intensities of these peaks are essentially higher for the O-18 sample at $T = 12$ K. In the neutron diffraction pattern of the O-16 sample at $T = 12$ K an increased contribution to the nuclear Bragg peaks (101)/(020) and (200)/(121) at $2\theta = 39^\circ$ and 56° , respectively, due to the ferromagnetic (FM) ordering, is clearly observed. The temperature dependencies of AFM and FM integrated peak intensities for both samples are displayed in Fig. 2. The intensity increases monotonically with decreasing temperature for the O-18 specimen. For the O-16 sample this dependence is nonmonotonic with a maximum at $T \approx 110$ K, which correlates with the appearance of FM a component in corresponding Bragg peaks. The intensity of the (101)/(020) peak for the O-16 sample displays [Fig. 2(b)] a small decrease below 50 K, which can be

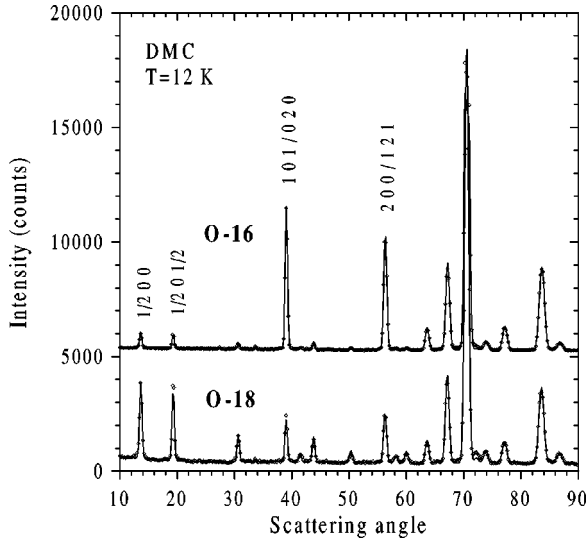


FIG. 1. Neutron diffraction patterns of the O-16 (top) and O-18 (bottom) samples measured on DMC at $T=12$ K. For the O-16 pattern the y scale is shifted by 5000 counts. The Miller indices highlight the most intensive AFM and FM peaks. At 12 K the AFM intensities of the $(\frac{1}{2}00)$ and $(\frac{1}{2}0\frac{1}{2})$ peaks are much higher for the O-18 sample, whereas for the O-16 sample the intensities of the FM peaks $(101)/(020)$ and $(200)/(121)$ are high.

interpreted as a result of magnetic ordering of Pr atoms similar to Refs. 20 and 4. For the O-18 sample, a FM contribution to the diffraction peaks is absent in the whole temperature range within the reached statistical accuracy of 1.3%.

For the O-16 sample the refinement of the magnetic structure was based on the model of two antiferromagnetic phases

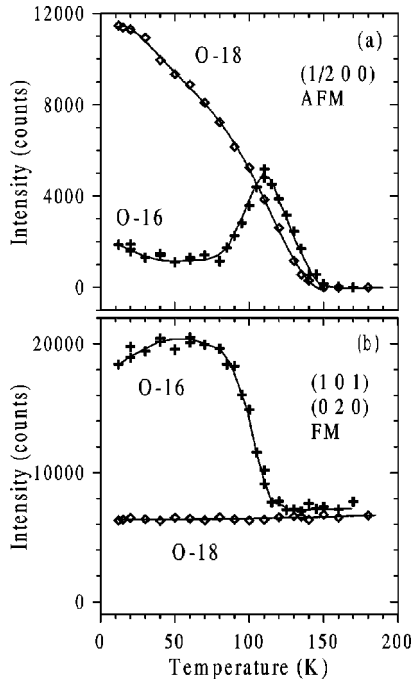


FIG. 2. Temperature dependencies of the integrated intensities for the characteristic neutron diffraction peaks of the O-16 and O-18 samples: (a) $(\frac{1}{2}00)$ AFM peak, (b) $(101)/(020)$ FM peaks. Decreasing of the $(101)/(020)$ intensities at $T < 40$ K for the O-16 sample is believed to be connected with the ferromagnetic ordering of Pr magnetic moments. The lines are guides to the eye.

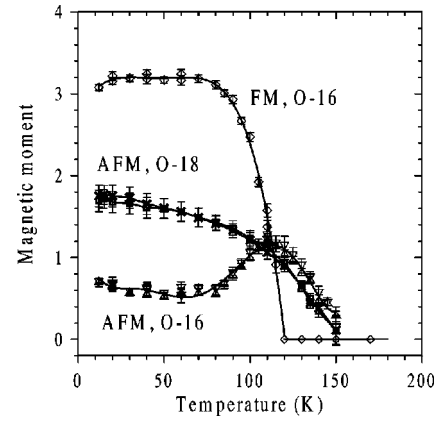


FIG. 3. Temperature dependencies of the Mn magnetic moments (in Bohr magnetons) for the FM and AFM components of the O-16 sample and for the AFM components of the O-18 sample. For the O-16 sample some of the points were measured twice. The values of the AFM moments for the O-18 sample for both propagation vectors coincide within the error bars. The lines are guides to the eye.

(AFM1 and AFM2) and a ferromagnetic phase with magnetic moments on the Mn atoms. The AFM1-phase peaks can be indexed using the $\mathbf{k}=(\frac{1}{2}00)$ or $\mathbf{k}=(00\frac{1}{2})$ propagation vectors (doubling of the a or c unit cell directions). The AFM2-phase peaks may be described using the $\mathbf{k}=(\frac{1}{2}0\frac{1}{2})$ propagation vector (both a and c parameters are doubled). The magnetic moments of manganese ions inside the chemical cell $2a \times b \times c$ for the AFM1 phase are $(+\mathbf{m})$ at $(0y\frac{1}{2})$, $(\frac{1}{4}y0)$; $(-\mathbf{m})$ at $(\frac{1}{2}y\frac{1}{2})$, $(\frac{3}{4}y0)$, where $y=0$ and $\frac{1}{2}$. For the phase AFM2 the magnetic moments inside the chemical cell $2a \times b \times 2c$ are $(+\mathbf{m})$ at $(0y\frac{1}{2})$, $(\frac{1}{4}y\frac{1}{2})$, $(\frac{1}{2}y\frac{3}{4})$, $(\frac{3}{4}y0)$; $(-\mathbf{m})$ at $(\frac{1}{2}y\frac{1}{4})$, $(\frac{3}{4}y\frac{1}{2})$, $(0y\frac{3}{4})$, $(\frac{1}{4}y0)$, where $y=0$ and $\frac{1}{2}$. The refinement of the magnetic structure of the O-18 sample was done in the same way, but without a FM component. Testing of different variants of moment orientation along the basic directions of the unit cell yielded the best agreement between measured and calculated intensities for the orientation of the Mn moment along the b axis in AFM phases, and along the c axis in the FM phase.

The temperature dependencies of the μ_{AFM1} , μ_{AFM2} , μ_{FM} magnetic moments are presented in Fig. 3. The values of the magnetic moments at low temperature in the O-16 sample do not exclude the possibility of a two-phase state. If we consider that the AFM phases in the O-16 sample have the same magnetic moments as the AFM phases in the O-18 sample then the fraction of the AFM phases in the O-16 sample, which is proportional to the square of the ratio of the magnetic moments, amounts to $\approx 15\%$. At this, the renormalized moment of the FM phase occupying the remaining 85% fraction amounts to $\approx 3.4\mu_B$, which does not exceed the reasonable magnetic moment of manganese ion. In the single-phase homogeneous picture the magnetic structure of the O-16 sample is a noncollinear canted structure, similar to those observed for $\text{Pr}_{0.7}\text{Ca}_{0.3}\text{MnO}_3$ (Ref. 4) and $\text{Pr}_{0.65}(\text{Ca}_{0.7}\text{Sr}_{0.3})_{0.35}\text{MnO}_3$.²¹ The complete suppression of the ferromagnetic component in the O-18 sample means that the isotope substitution does not lead to a simple shift of transi-

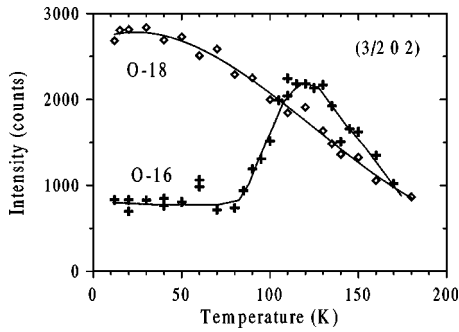


FIG. 4. Temperature dependencies of the $(\frac{3}{2}02)$ CO peak integrated intensity for the O-16 and O-18 samples. At room temperature this peak is absent. For the O-16 sample some of the points were measured twice. The lines are guides to the eye.

tion temperature in the magnetic phase diagram $T_{FM}(\langle r_A \rangle)$, but results in a completely new magnetic state. This type of ordering has not been observed before in Pr manganites with 30% doping level and natural oxygen isotope content.

In both samples, the appearance of weak superlattice reflections of $(\frac{3}{2}02)$ type at $T_{CO} \approx 180$ K (Fig. 4) precedes AFM ordering ($T_{AFM} = 150$ K). The appearance of these reflections is believed to be connected to the charge ordering of Mn^{3+}/Mn^{4+} cations, leading to the doubling of the a axis and lowering of the symmetry to the monoclinic $P2_1/m$ space group.²² This effect was thoroughly studied in $Pr_{0.7}Ca_{0.3}MnO_3$ (Refs. 4,23) and $La_{0.5}Ca_{0.5}MnO_3$ compositions.²² The synchronism in temperature behavior of the intensities of the CO and AFM peaks of the O-16 sample could indicate in favor of segregation on AFM insulating and FM metallic phases at low temperature, though no direct indications of long-range phase segregation were found.

The temperature dependencies of the unit cell parameters for both samples were measured on the HRFD instrument in Dubna, whose high resolution ($\Delta d/d = 0.0015-0.0018$ in the working range of d spacing 0.6–3.5 Å) allowed to obtain high precision data. Several distinctive features are easily seen in the dependencies presented in Fig. 5 which correlate with behavior of the magnetic structure and the electrical properties. In both samples the temperature dependencies of the unit cell parameters are identical between room temperature and the transition temperature of the O-16 sample to the metallic state. Moreover, their absolute values are practically the same. Any anomalies of the behavior of unit cell volume are absent, although the a and b parameters have nonlinear dependencies close to the T_{CO} charge ordering temperature. A similar behavior of a and b parameters was found and qualitatively interpreted by Cox *et al.*⁴ for the $Pr_{0.7}Ca_{0.3}MnO_3$ compound. Antiferromagnetic ordering at $T_{AFM} = 150$ K is not revealed in the temperature dependencies of the lattice parameters, but the b parameter, and to some extent, the c parameter of the O-16 sample have well observed sharp jumps at $T_{FM} = 110$ K, which is also well visible in the unit cell volume $V_c(T)$ dependence. This behavior corresponds to the transition from a high-volume to a low-volume state at the phase transition from the insulating to the metallic state as was pointed out in Ref. 14. In contrast to Ref. 4, we did not observe significant effects of diffraction peak broadening, in spite of the high resolution of the HRFD

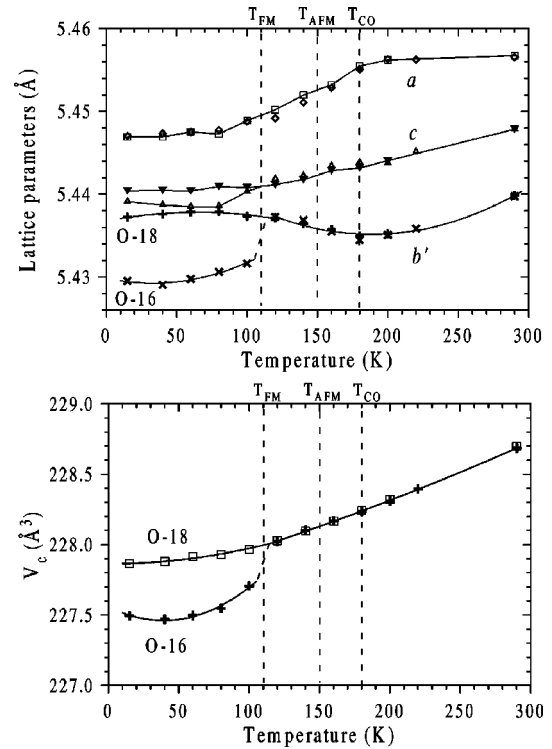


FIG. 5. Temperature dependencies of lattice parameters (top) and of unit cell volume (bottom) for the O-16 and O-18 samples. Between T_{FM} and room temperature, there is practically no difference between the parameters of the samples. The solid lines are guides to the eye.

instrument. Small peak broadening (at a level of 10%) was observed in the temperature range from 110 K to 200 K for the O-16 sample, i.e., between T_{FM} and T_{CO} , whereas the O-16 and O-18 samples' peak widths are identical at room and $T < T_{FM}$ temperatures. It means that in both samples we have no direct evidence for long-range phase segregation, though the behavior of magnetic moments and of CO-peak intensities versus temperature supports a suggestion of its appearance below T_{FM} . Also, we cannot exclude liquidlike ferromagnetic clusters as discussed in Ref. 24.

In conclusion, important new results of the neutron diffraction study of two $(La_{0.25}Pr_{0.75})_{0.7}Ca_{0.3}MnO_3$ samples enriched by oxygen ^{16}O and ^{18}O isotopes, respectively, are presented. It is shown that at room temperature the samples are structurally identical. Below $T = T_{CO} \approx 180$ K, charge ordering develops in both samples. Antiferromagnetic ordering of manganese magnetic moments is observed below $T = T_{AFM} = 150$ K with propagation vectors $(\frac{1}{2}00)$ or $(00\frac{1}{2})$ and $(\frac{1}{2}0\frac{1}{2})$. CO and AFM ordering processes are developed identically in both samples down to 110 K. Below $T_{FM} = 110$ K the magnetic structure changes in the O-16 sample, leading to the appearance of a FM component, decreasing of AFM components, and partial destroying of the charge ordered state, while the O-18 sample remains AFM and charge ordered. We emphasize that oxygen isotope substitution did not affect T_{CO} and T_{AFM} . We did not find any traces of long-range phase segregation in the O-16 sample at low temperature. The width of diffraction peaks and the saturation

value of the manganese magnetic moments show that the samples may be macroscopically uniform, while the synchronism in temperature behavior of the intensities of the $(\frac{1}{2}00)$ and $(\frac{3}{2}02)$ peaks could indicate in favor of phase segregation of the O-16 sample on AFM-insulating and FM-metallic phases. These results prove that the low temperature state of the $(\text{La}_{0.25}\text{Pr}_{0.75})_{0.7}\text{Ca}_{0.3}\text{MnO}_3$ is indeed governed by strong electron-phonon interaction. And thus we suggest that the sole variation of oxygen mass is responsible for both the change of the electronic state (metal-insulator) and remark-

able alteration of the magnetic state (noncollinear ferromagnetic–pure antiferromagnetic).

The authors are grateful to A. V. Pole and V. G. Simkin for help in the neutron diffraction experiment at HRFD, to V. A. Amelichev, A. A. Bosak, and E. A. Chistotina for help in the sample preparation and characterization and E. V. Raspopina for aid in preparation of the manuscript. This study was supported by the Russian Foundation for Basic Research (Grant Nos. 96-02-17823, 97-02-16665, 96-15-96738, and 97-03-32979a) and the INTAS-RFBF program (Grant Nos. I-96-0639, IR-97-1954, and I-97-0963).

*Present address: Laboratory for Neutron Scattering, ETH Zürich and Paul Scherrer Institute, CH-5232 Villigen PSI, Switzerland.

¹S. Jin, M. McCormack, T. H. Tiefel, and R. Ramesh, *J. Appl. Phys.* **76**, 6929 (1994).

²C. N. R. Rao, A. K. Cheetham, and R. Mahesh, *Chem. Mater.* **8**, 2421 (1996).

³A. P. Ramirez, *J. Phys.: Condens. Matter* **9**, 8171 (1997).

⁴D. Cox, P. G. Radaelli, M. Marezio, and S.-W. Cheong, *Phys. Rev. B* **57**, 3305 (1998).

⁵A. J. Millis, *Nature (London)* **392**, 147 (1998).

⁶G. M. Zhao, K. Conder, H. Keller, and K. A. Müller, *Nature (London)* **381**, 676 (1996).

⁷G. M. Zhao, M. B. Hunt, and H. Keller, *Phys. Rev. Lett.* **78**, 955 (1997).

⁸G. M. Zhao, H. Keller, J. Hofer, A. Shengelaya, and K. A. Müller, *Solid State Commun.* **104**, 57 (1997).

⁹N. A. Babushkina, L. M. Belova, O. Yu. Gorbenko, A. R. Kaul, A. A. Bosak, V. I. Ozhogin, and K. I. Kugel, *Nature (London)* **391**, 159 (1998).

¹⁰N. A. Babushkina, L. M. Belova, V. I. Ozhogin, O. Yu. Gorbenko, A. R. Kaul, A. A. Bosak, D. I. Khomskii, and K. I. Kugel, *J. Appl. Phys.* **83**, 7369 (1998).

¹¹I. Isaac and J. P. Franck, *Phys. Rev. B* **57**, R5602 (1998).

¹²J. P. Frank, I. Isaac, W. Chen, J. Chrzanowski, and J. C. Irwin, *Phys. Rev. B* **58**, 5189 (1998).

¹³B. Carcia-Landa, M. R. Ibarra, J. M. De Teresa, G. M. Zhao, K.

Konder, and H. Keller, *Solid State Commun.* **105**, 567 (1998).

¹⁴M. R. Ibarra, G. M. Zhao, J. M. De Teresa, B. Garcia-Landa, Z. Arnold, C. Marquina, P. A. Algarabel, H. Keller, and C. Ritter, *Phys. Rev. B* **57**, 7446 (1998).

¹⁵A. M. Balagurov, V. Yu. Pomjakushin, V. L. Aksenov, N. M. Plakida, N. A. Babushkina, L. M. Belova, O. Yu. Gorbenko, A. R. Kaul, P. Fischer, M. Gutmann, and L. Keller, *Pis'ma Zh. Éksp. Teor. Fiz.* **67**, 672 (1998) [*JETP Lett.* **67**, 705 (1998)].

¹⁶J. Rodrigues-Carvajal, *Physica B* **192**, 55 (1993).

¹⁷V. L. Aksenov, A. M. Balagurov, V. G. Simkin, A. P. Bulkin, V. A. Kudryashev, V. A. Trounov, O. Antson, P. Hiimaki, and A. Tiitta, *J. Neutron Res.* **5**, 181 (1997).

¹⁸C. Ritter, M. R. Ibarra, J. M. De Teresa, P. A. Algarabel, C. Marquina, J. Blasco, J. Garcia, S. Oseroff, and S.-W. Cheong, *Phys. Rev. B* **56**, 8902 (1997).

¹⁹I. G. Krogh Andersen, E. Krogh Andersen, P. Norby, and E. Skou, *J. Solid State Chem.* **113**, 320 (1994).

²⁰Z. Jirak, S. Vratilav, and J. Zajicek, *Phys. Status Solidi A* **52**, K39 (1979).

²¹H. Yoshizawa, R. Kajimoto, H. Kawano, Y. Tomioka, and Y. Tokura, *Phys. Rev. B* **55**, 2729 (1997).

²²P. G. Radaelli, D. E. Cox, M. Marezio, and S.-W. Cheong, *Phys. Rev. B* **55**, 3015 (1997).

²³H. Yoshizawa, H. Kawano, Y. Tomioka, and Y. Tokura, *Phys. Rev. B* **52**, R13 145 (1995).

²⁴M. Hennion, F. Moussa, G. Biotteau, J. Rodriguez-Carvajal, L. Pinsard, and A. Revcolevschi, *Phys. Rev. Lett.* **81**, 1957 (1998).